Materials Science & Engineering A 619 (2014) 205–211

Contents lists available at ScienceDirect

Materials Science & Engineering A

journal homepage: www.elsevier.com/locate/msea

Ultrahigh strength-ductility steel treated by a novel quenching–partitioning–tempering process

Ke Zhang [a,*], Ping Liu [a], Wei Li [a], Zhenghong Guo [b], Yonghua Rong [b]

[a] School of Materials Science and Engineering, University of Shanghai for Science and Technology, Shanghai 200093, China
[b] School of Materials Science and Engineering, Shanghai Jiao Tong University, Shanghai 200240, China

ARTICLE INFO

Article history:
Received 22 June 2014
Received in revised form
25 September 2014
Accepted 27 September 2014
Available online 5 October 2014

Keywords:
Ultrahigh strength-ductility steel
Quenching–partitioning–tempering process
X-ray diffraction
Transmission electron microscopy
Electron backscatter diffraction

ABSTRACT

A novel quenching–partitioning–tempering (Q–P–T) process was employed in two kinds of Fe–Mn–Si–Nb alloyed steels with 0.2 wt% and 0.4 wt% carbon additions to obtain a triplex microstructure comprising martensite, retained austenite and fine carbides. The good combination of strength and elongation has been realized for Fe–Mn–Si–Nb alloyed Q–P–T steels. The product of strength and elongation is high up to 31.4 GPa% for Q–P–T steel with 0.4 wt% carbon (Ultimate tensile strength: ~1549 MPa; Elongation: ~20.3%), which meets the mechanical properties theoretically predicted of next generation advanced high strength steel. The strength and ductility both enhance with increase of carbon content in Q–P–T steels. Two possible mechanisms are employed to explain the reason of good mechanical properties.

1. Introduction

In recent decades, the trend of developing advanced high-strength steels (AHSS) from dual phase (DP) steels [1], transformation induced plasticity (TRIP) steels [2–4], twinning induced plasticity (TWIP) steels [5], quenching & partitioning (Q&P) steels [6–10] to quenching–partitioning–tempering (Q–P–T) steels [11,12] is the combination of higher strength and adequate ductility for saving energy and raw materials as well as environment protection. In AHSS, martensitic steels exhibit the highest strength. The martensitic steels treated by Q&P process, which was proposed by Speer et al. [6,7], demonstrate excellent combination of high strength and adequate ductility. Q&P process involves a fast quenching to a desired temperature (T_q) between the martensite-start (M_s) and martensite-finish (M_f) temperatures, followed by a partitioning step at or above the T_q with the purpose of promoting the partitioning of carbon from the supersaturated martensite into austenite, thereby the enriched-carbon retained austenite keeps stable during subsequent cooling to ambient temperature. In early Q&P steels, Si and/or Al were added to suppress the competition of carbon partitioning and carbide precipitation, ensuring the best effect of austenite stabilization. Consequently, the carbide formation elements (e.g. Nb, Mo and V) were eliminated from Q&P steels, which excluded the potential strengthening manners of grain refinement and carbide precipitation. In order to explore the effect of precipitation strengthening and further improve mechanical properties, Hsu [13] proposed a novel Q–P–T process as a modified Q&P one. The carbide formation elements were added into Q–P–T steel instead of eliminating them. The presence of fine carbides during tempering step further enhanced the strength of Q–P–T steel. In Q–P–T process, a proper T_q is determined according to a constrained carbon paraequilibrium (CCE) theory [10] and Koistinen–Marburger (K–M) relationship [14], so the maximum fraction of retained austenite can be also obtained. Earlier experimental results demonstrated that Fe–Mn–Si–Nb alloyed steels subjected to Q–P–T process exhibited better combination of strength and elongation comparing with Q&P steels [11,12].

Matlock and Speer [15] predicted the relationship between tensile strength and uniform elongation for the next generation AHSS based on Mileiko model [16]. For example, the tensile strength of 1500 MPa corresponds to the uniform elongation of about 12%, as a result, the product of strength and elongation (PSE) will reach about 30 GPa% if the elongation after necking is considered as about 8%. The AHSS with PSE over 30 GPa% has rarely been reported except for high-Mn TWIP steels [17]. The present work intends to develop a Q–P–T steel with PSE over 30 GPa% and reveal the mechanism of such a ultrahigh strength-ductility Q–P–T steel by microstructural characterization.

2. Experimental procedure

Two steels (abbreviated as Fe–0.2C and Fe–0.4C) were melted in a laboratory medium frequency furnace and hot-rolled to

* Corresponding author. Tel./fax: +86 21 55270943.
E-mail address: zhangke@usst.edu.cn (K. Zhang).

http://dx.doi.org/10.1016/j.msea.2014.09.100
0921-5093/

Table 1
Chemical compositions of experimental Q–P–T steels (wt%).

Sample	C	Mn	Si	Nb	Ac_3 (°C)	M_s (°C)	M_f (°C)	Optimal T_q (°C)
Fe–0.2C	0.19	1.52	1.57	0.029	911 ± 5	395 ± 5	171 ± 3	316
Fe–0.4C	0.42	1.46	1.58	0.028	797 ± 5	289 ± 5	84 ± 3	224

12 mm thickness. The chemical compositions of the experimental steels are listed in Table 1. The austenite finishing (Ac_3) temperature during the heating cycle together with the M_s and M_f temperatures, was measured in cylindrical dilatometric samples of diameter 3 mm and length 10 mm using a Formaster FII dilatometer. The optimal T_q was calculated to be 316 °C for Fe–0.2C sample, 224 °C for Fe–0.4C sample based on CCE theory and K–M relationship. The samples with thickness of 2 mm were cut from a hot-rolled plate for Q–P–T process. The samples were austenitized (960 °C for Fe–0.2C, 850 °C for Fe–0.4C) for 300 s, followed by quenching into salt bath (300 °C for Fe–0.2C, 200 °C for Fe–0.4C) for 15 s and subsequent both partitioning/tempering at 450 °C for 30 s in molten salt, then quenching to room temperature.

Standard tensile specimens with a gage length of 15 mm and width of 5 mm were used for tensile testing on Zwick T1-FR020TN A50 tensile testing machine with a strain rate of $10^{-3}\,s^{-1}$. The tensile axis was selected along the rolling direction. X-ray diffractometry (XRD, D/MAX-2550 X-ray, CuKα radiation) was used to determine the volume fraction of retained austenite. The volume fraction of retained austenite (V_{RA}) was calculated using a direct comparison method [18] from the integrated intensities of austenite peaks $(200)_\gamma$, $(220)_\gamma$, $(311)_\gamma$ and martensite ones $(200)_\alpha$, $(211)_\alpha$. The electron backscatter diffraction (EBSD) samples were prepared by mechanically polishing and then electropolishing in 7% perchloric acid and 93% ethanol. The orientation maps were obtained with a beam step of 0.05 μm by a scanning electron microscope (SEM, Zeiss Super55, 20 kV) equipped with an FE–type gun and EBSD HKL system with Channel 5 software. The microstructure of the steels was further characterized by transmission electron microscopy (TEM, JEM-2100F, 200 kV) after electropolishing with a twin-jet polisher in 4% perchloric acid and 96% ethanol solution at −20 °C.

3. Results

3.1. Mechanical properties

Fig. 1 shows the engineering stress–strain curves of Fe–0.2C and Fe–0.4C specimens treated by Q–P–T process. The mechanical properties of all specimens studied, such as yield strength ($R_p0.2$), ultimate tensile strength (R_m), uniform elongation (A_{gt}), total elongation (A) and the product of tensile strength and elongation (PSE, $R_m \times A$) are summarized in Table 2. For each steel composition and treated state, three specimens were used in tension test. The results indicate that the samples subjected to Q–P–T process exhibit high strength and adequate elongation. For example, Fe–0.2C samples possess the ultimate tensile strength of 1215 MPa and elongation of 15.2% (uniform elongation of 6.0%) and Fe–0.4C samples possess the ultimate tensile strength of 1549 MPa and elongation of 20.3% (uniform elongation of 12.2%). Compared with Fe–0.2C samples, the Fe–0.4C samples exhibit a better combination of strength and elongation, i.e. the PSE reaches 31.4 GPa%, which exceeds the predicted value of the next generation AHSS proposed by Matlock and Speer.

3.2. XRD measurement of retained austenite volume fraction

Fig. 2 shows the XRD spectra of Fe–0.2C and Fe–0.4C samples treated by Q–P–T process. As demonstrated in Fig. 2, Q–P–T

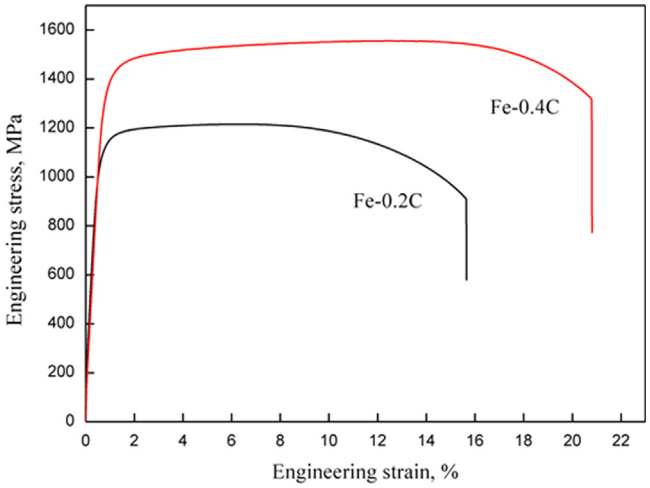

Fig. 1. Engineering stress–strain curves of Fe–0.2C and Fe–0.4C Q–P–T samples.

Table 2
The mechanical properties of the Fe–0.2C and Fe–0.4C Q–P–T specimens.

Sample	$R_{p0.2}$/MPa	R_m/MPa	A_{gt}/%	A/%	PSE/GPa%
Fe–0.2C	1092 ± 11	1215 ± 14	6.0 ± 0.2	15.2 ± 0.2	18.5
Fe–0.4C	1348 ± 15	1549 ± 15	12.2 ± 0.3	20.3 ± 0.2	31.4

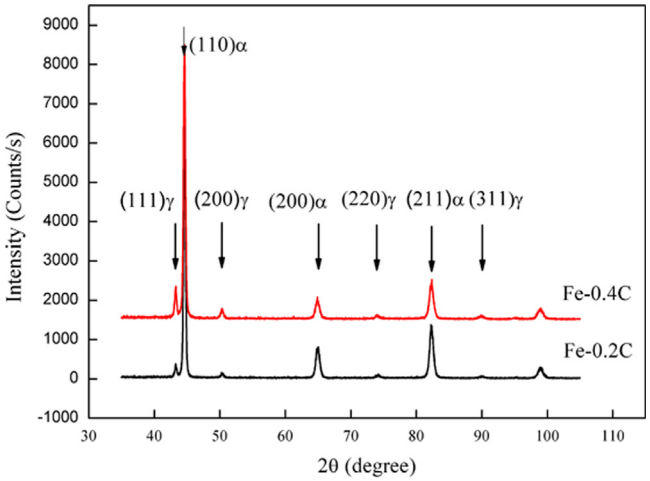

Fig. 2. XRD spectra of Fe–0.2C and Fe–0.4C Q–P–T samples.

samples contain martensite and retained austenite. The V_{RA} was calculated based on XRD spectra, which increases with the increase of carbon content, i.e. 6.5% for Fe–0.2C sample and 16% for Fe–0.4C sample. In order to clarify the effect of retained austenite on ductility, the V_{RA} as a function of engineer strain (from 0%, 3%, 7%, 11%, 15% to 19%) for Fe–0.4C Q–P–T samples were further calculated and the results are plotted in Fig. 3. The V_{RA} decreases with the increase of engineering strain until it cannot be measured at 19% strain, which shows the retained austenite transformed into martensite.

3.3. Microstructural characterization by TEM

The TEM investigations of the Fe–0.2C and Fe–0.4C samples treated by Q–P–T process are illustrated in Fig. 4. It is clearly shown that the present Q–P–T samples have the identical microstructure: dislocation-type martensite laths and flake-like retained austenite located between martensite laths. Comparing Fig. 4b